Centre de Recherches Mathématiques
CRM Proceedings and Lecture Notes
Volume **41**, 2007

A Maxwell–Schrödinger Model for Non-perturbative Laser-molecule Interaction and Some Methods of Numerical Computation

E. Lorin, S. Chelkowski, and A. Bandrauk

Abstract. We present in this paper a numerical Maxwell–Schrödinger model to simulate intense ultrashort laser pulses interacting with a H_2^+-gas in the nonlinear non-perturbative regime. After presentation of the model and a short mathematical study, we propose a numerical approach for its computation. In particular we focus on the polarization computation allowing the coupling between the Maxwell and Schrödinger equations, and on the boundary conditions problem for the time dependent Schrödinger equations, TDSE. Some comparisons with existing methods are also addressed.

1. Introduction

From the theoretical point of view to the very practical point of view (controlled fusion by inertial confinement [13], quantum dynamic imaging [6], attosecond pulse generation [1], filamentation [27]), there exist numerous applications of ultrashort and intense laser pulses. Indeed current laser technology allows to create ultrashort pulses with intensities exceeding molecular and atomic internal electric fields. Typically, for the hydrogen atom the period of electron circulation is 24.6×10^{-18}s (attosecond) and the intensity of its Coulomb field is $3.5 \times 10^{16}\mathrm{W/cm}^2$. Current laser intensities can reach around $10^{20}\mathrm{W/cm}^2$ with pulse durations of ~ 150 attoseconds. The main goal of this work is to study high order non-perturbative nonlinear phenomena: ATI (Above Threshold Ionization), HOHG (High Order Harmonic Generation) [12], obtained with very intense lasers interacting with molecules and to study their dynamics. HOHG is one of these nonlinear phenomena that appears when the electric field is greater than the Coulomb potential field and leads to ionization. It is, moreover, the current source of coherent "attosecond" pulses [1, 11]. In a first step the electron is excited by an intense electric field and then leaves through tunnelling the ion vicinity and enters in the ionized continuum with an initial velocity equal to zero [12]. Then the free electron is accelerated by the strong electric field and gains energy. In a last step the electron is driven back to the vicinity of the parent ion and recombines with it, leading to the creation of

2000 *Mathematics Subject Classification.* Primary: 65Z05, 81V10; Secondary: 65Y05, 81V55.

This is the final form of the paper.

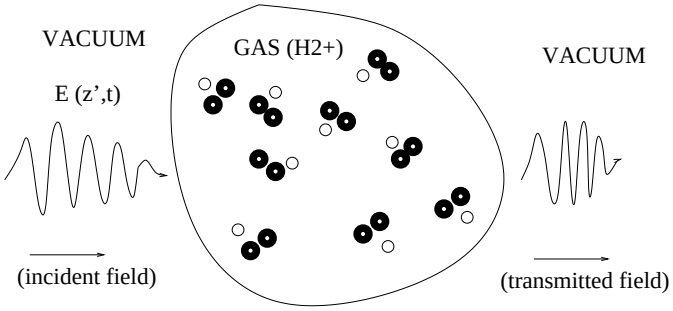

FIGURE 1. Laser-molecule interactions in a H_2^+ gas.

high order harmonics (see [24] for description of HOHG or [17] for their numerical aspects).

In this paper we will introduce a precise numerical model to describe this dynamics, including ionization, dissociation of the molecule and including propagation effects in order to take into account phase matching [12]. We propose here to study ultrashort pulses interacting with one electron H_2^+-molecules. To model the nonlinear response, the most natural way is to consider a coupling between the Maxwell equations describing the behavior of the electric and magnetic fields and the time dependent Schrödinger equation (TDSE) describing the electron motions and ionization. In order to increase the precision of the model, we propose to go beyond the Born–Oppenheimer approximation taking into account the proton motions. The Maxwell and the Schrödinger equations are then coupled with the polarization of molecules that describes the relative position of all the particles constituting the molecule. The model is written first in its whole generality and then some approximations are proposed in order to solve it numerically. Note that the model we propose although close to the atomic models presented in [28, 29] (see also [15, 16]) includes both electron and nuclear motion. The present work is the first to treat molecules completely.

In Section 2. we will present our model and we will briefly evoke some other existing ones. Then we will focus on the existence of solutions for the TDSE we consider. Finally in a last part we will give a simple presentation of the numerical method we have used to solve the coupled system. In particular we will detail the polarization computation (and how to reduce it in CPU time) and on the numerical boundary conditions for the TDSE, crucial in this framework. In [25] an exhaustive presentation of both the model and numerical approach will be proposed in a real 3-D configuration.

2. Mathematical Modeling

There exist many models describing the laser-matter interaction problems described above. The simplest ones are the *nonlinear Maxwell models*, and consist in calculating the polarization as an expansion of the susceptibility (linear, quadratic, cubic, and so on):

$$P(z',t) = \chi^{(1)} \cdot E + \chi^{(2)} \cdot E^2 + \chi^{(3)} \cdot E^3 + \cdots , \tag{2.1}$$

where $\chi^{(i)}$ are the nonlinear polarizabilities (susceptibilities) [12]. Some slowly varying envelope (SVE) versions leading to nonlinear TDSE, also exist. These models allow for example to simulate the behavior of low intensity lasers with low order harmonic generation. As the transmitted fields possess high order harmonics at high intensities these models are in fact not valid here as they do not include ionization. The Maxwell–Bloch equations constitute a more precise model where the polarization is obtained from the TDSE *via* the Bloch equation coupled with the Maxwell equations. The polarization is then deduced from the Bloch equation (ODE for the density matrix).

Unfortunately with such a model it is *a priori* not possible to include the continuous part of the Hamiltonian (ionization) and therefore it is not adapted to compute high order harmonics with very intense laser pulses (typically of the order of the Coulomb potential intensity). Such a strong approximation induces then a "loss of informations" hard to evaluate. Details can be found in [26].

The Maxwell–Schrödinger model we consider is then much more precise than the usual models briefly presented above in the sense that it considers much more physical phenomena in the non-perturbative regime where the continuous spectrum must be included. Furthermore, we propose to include nuclear motion thus allowing to go beyond the Born–Oppenheimer approximation and take into account dissociative ionization [7].

2.1. Presentation of the Maxwell–Schrödinger model. The 3-D TDSE describing the H_2^+ molecule response excited by a laser field is given by [7]:

$$i\partial_t\psi(\mathbf{r},R,\mathbf{r}',t) = \left[-\frac{1}{2}\triangle_{\mathbf{r}} + V_c(\mathbf{r},R) - \frac{i}{c}\mathbf{A}(\mathbf{r}',t)\cdot\boldsymbol{\nabla}_{\mathbf{r}} + V_i(R) - \frac{1}{m_p}\partial^2_{RR} + \frac{\|\mathbf{A}(z',t)\|^2}{2c^2}\right]\psi(\mathbf{r},R,\mathbf{r}',t), \tag{2.2}$$

where ψ represents the wave function, m_p denotes the H^+ mass. The Coulomb and nuclear potentials are given by:

$$V_c(\mathbf{r},R) = -\frac{1}{\sqrt{x^2+(y-R/2)^2+z^2}} - \frac{1}{\sqrt{x^2+(y+R/2)^2+z^2}}, \qquad V_i(R) = \frac{1}{R}. \tag{2.3}$$

We use atomic units, where $e = h/2\pi = m_e = 1$ and $m_p = 1837$ and $c = 137$. The electron position in the ion center of mass coordinates is denoted by $\mathbf{r} = (x,y,z)^T$. R represents the proton relative position. We assume in this paper that the ion motion R, is 1-D. The term $\mathbf{A}\cdot\boldsymbol{\nabla} + \|\mathbf{A}\|/2c^2$ denotes the field interaction, $\mathbf{A}$ being the vector potential, and $\mathbf{r}'$ denotes the field space variable. In the following we will suppose that the electric field propagation is 1-D (in the direction z') and polarized in the direction y, so that the TDSE becomes (see Fig. 2):

$$i\partial_t\psi(\mathbf{r},R,z',t) = \left[-\frac{1}{2}\triangle_{\mathbf{r}} + V_c(\mathbf{r},R) - \frac{i}{c}A_{y'}(z',t)\partial_y + V_i(R) - \frac{1}{m_p}\partial^2_{RR} + \frac{|A_{y'}(z',t)|^2}{2c^2}\right]\psi(\mathbf{r},R,z',t). \tag{2.4}$$

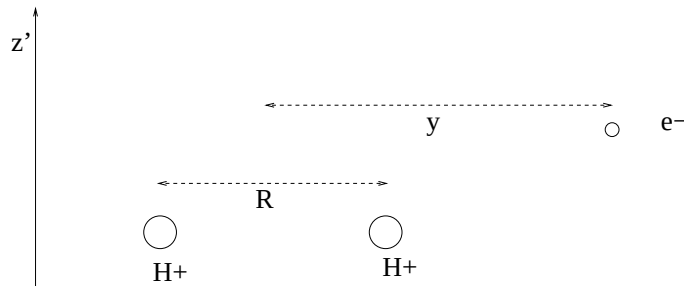

FIGURE 2. Coordinates.

Note that in our coordinates, $\mathbf{e}_y \cdot \mathbf{e}_{z'} = 0$, $\mathbf{e}_z = \mathbf{e}_{z'}$, $\mathbf{e}_y = \mathbf{e}_{y'}$ and $A_{y'}$ is the y'-component of $\mathbf{A}$. Now, if the laser wavelength λ, is large enough we can assume that the electric and magnetic fields are constant in space at the molecular scale ℓ, $(\lambda/\ell \ll 1)$, allowing us to reduce the numerical and mathematical complexity of the problem. Indeed, in this situation the TDSE can be written in its dipole form[1]:

$$i\partial_t \psi_{z'}(\mathbf{r}, R, t) = \left[-\frac{1}{2}\triangle_{\mathbf{r}} + V_c(\mathbf{r}, R) - \frac{iA_{y',z'}(t)}{c}\partial_y + V_i(R) \right. \\ \left. -\frac{1}{m_p}\partial^2_{RR} + \frac{|A_{y',z'}(t)|^2}{2c^2} \right] \psi_{z'}(\mathbf{r}, R, t), \tag{2.5}$$

z' is now a parameter denoting the molecule position in the "Maxwell domain". For each z' in the gas, one has to solve a 4D-TDSE (3-D for the electron and 1-D for the proton). Let us remark that the dipole approximation leads to $[\triangle_{\mathbf{r}}, A_{y',z'}(t)\partial_y] = [\partial^2_{RR}, A_{y',z'}(t)\partial_y] = 0$; very useful feature to have a free error numerical splitting method based on this commutation.

The above TDSE is given is the so-called *velocity gauge* where the electron-field interaction is through the electron momentum $p_y = i\partial/\partial_y$. Another possible formulation is in the so-called *length gauge*, see [7]. Setting

$$\psi \mapsto \psi \exp\left(\frac{i}{2c^2} \int_0^t |A_{y',z'}|^2(s)\, ds + \frac{i}{c} y A_{y',z'}(t) \right), \tag{2.6}$$

we get a new formulation of the TDSE:

$$i\partial_t \psi_{z'}(\mathbf{r}, R, t) = \left[-\frac{1}{2}\triangle_{\mathbf{r}} + V_c(\mathbf{r}, R) + yE_{y',z'}(t) + V_i(R) \right. \\ \left. -\frac{1}{m_p}\partial^2_{RR} \right] \psi_{z'}(\mathbf{r}, R, t). \tag{2.7}$$

with $cE_{y',z'}(t) = -\partial A_{y',z'}(t)/\partial t$ denoting the electric field. The interaction with the electric field is now through the electron dipole y.

Ideally the electric field dynamics modeling is given by the microscopic Maxwell equations where the molecular density $n = n(\mathbf{r}', t)$, coupled with the TDSE and will be done in a future work. A full description of the microscopic Maxwell equations can be found in [20].

An approximate approach is proposed in [22], where the authors study the microscopic Maxwell equations but coupled with classical dynamics equations to

[1]The notation $A_{y',z'}$ denotes that z' is a parameter of the y'-component of $\mathbf{A}$.

describe the particle motions. We will here consider the macroscopic Maxwell equations that correspond to a spatial average of the microscopic ones. These equations are typically valid in a domain equal or exceeding a size of 10^{-18}cm^3 with a sufficiently high molecular density (see again [20]). The macroscopic 3-D-Maxwell equations written in atomic units are:

$$\begin{cases} \partial_t \mathbf{B} = -c\nabla \times \mathbf{E}, \\ \partial_t \mathbf{E} = c\nabla \times \mathbf{B} - 4\pi \partial_t \mathbf{P}, \\ \nabla \cdot \mathbf{B} = 0, \\ \nabla \cdot (\mathbf{E} + 4\pi \mathbf{P}) = 0. \end{cases} \tag{2.8}$$

We consider here a 1-D propagation (direction $\mathbf{e}_{z'}$ orthogonal to $\mathbf{e}_y$) with c denoting the light velocity in the vacuum and we neglect the transversal effects (justified in a gas due to large inter-molecular distances). We then have $\mathbf{E} = E_{y'}\mathbf{e}_{y'}$, $\mathbf{P} = P_{y'}\mathbf{e}_{y'}$ and $\mathbf{B} = B_x \mathbf{e}_{x'}$. Denoting $E = E_{y'}$, $P = P_{y'}$ and $B = B_{x'}$, we have the simple equations (the fields are not independent of x' and y'):

$$\begin{cases} \partial_t B(z',t) = c\partial_t E(z',t), \\ \partial_t E(z',t) = c\partial_t B(z',t) - 4\pi \partial_t P(z',t). \end{cases}$$

Under the dipolar approximation the polarization P for a molecule located at z' is effectively parallel to $\mathbf{e}_{y'}$ and is given by:

$$P(z',t) = -n(z') \int \psi_{z'}(\mathbf{r},R,t) y \psi^*_{z'}(\mathbf{r},R,t)\, dR\, d\mathbf{r}, \tag{2.9}$$

and the dipolar acceleration is

$$d(z',t) = -n(z') \int \psi_{z'}(\mathbf{r},R,t) \left(\frac{\partial V}{\partial y} + E(t) \right) \psi^*_{z'}(\mathbf{r},R,t)\, dR\, d\mathbf{r}, \tag{2.10}$$

where $n(z')$ denotes the molecular density given for example for all x' and y', by:

$$n(z') = \begin{cases} 0, & \text{if } \ell < |z'| < L, \\ n_0 \sin^2\left(\dfrac{\pi(|z'| - \ell)}{2(a-\ell)} \right) & \text{if } a < |z'| < \ell, \\ n_0 & \text{if } |z'| < a, \end{cases} \tag{2.11}$$

where $n_0 \in \mathbb{R}^*_+$ (mol/cm^3). Such a density choice will allow us in particular to numerically reduce the reflections of the incoming electric field at the "frontiers" of the gas.

We assume now, that the Maxwell computational domain is given by $[-L, L]$, $L > 0$. We introduce some real constants ℓ, a such that $L > \ell > a > 0$, where the molecules are located in $[-\ell, \ell]$, and the vacuum region is $[-L, -\ell] \cup [\ell, L]$. Initially for the laser-pulse of frequency ω, the electric field is defined as follows:

$$\begin{cases} E(z',0) = E_0(z') f_\omega(z'), & z' \in [-L, -\ell],\ \omega \in \mathbb{R}^*_+, \\ E(z',0) = 0, & \text{elsewhere.} \end{cases} \tag{2.12}$$

Where $\int E(t)\, dt = 0$.

The function f, usually a sinusoidal function, and E_0, the envelope, is a Gaussian function $E_0(z') = e^{-c_z(z'-z_c)^2}$, where z_c is the molecule center of mass and c_z a positive constant depending on the pulse radius. In fact this function should depend on x' and y' ($E_0(x',y',z') = e^{-c_x(x'-x_c)^2 - c_y(y'-y_c)^2 - c_z(z'-z_c)^2}$) but in most

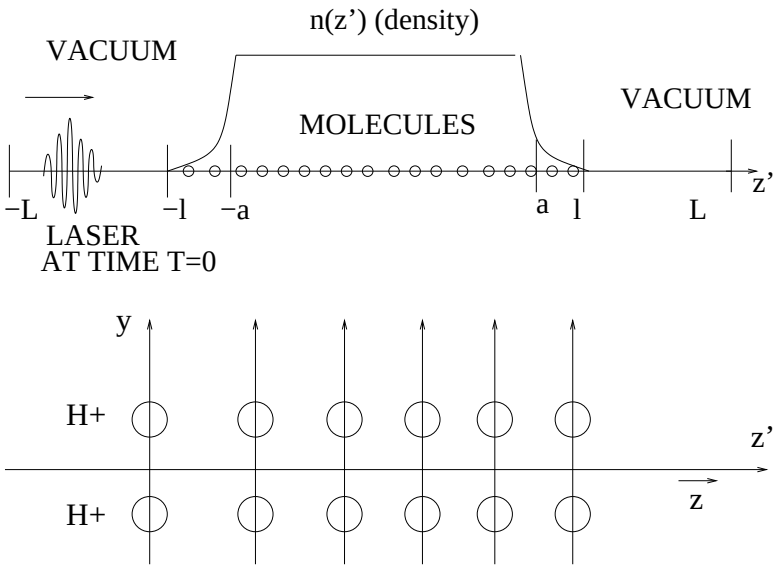

FIGURE 3. Physical configuration

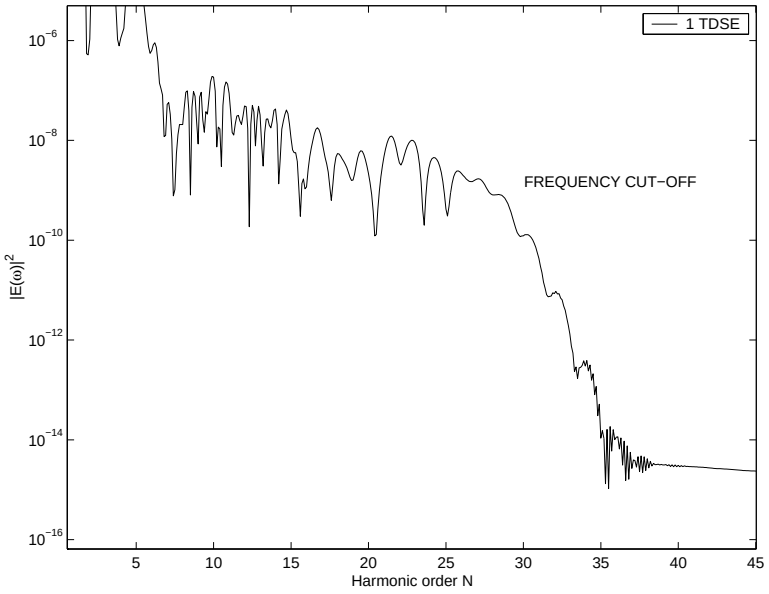

FIGURE 4. $|\widehat{E}(\omega)|^2$, for a single molecule, and a 5-cycle laser pulse at $I = 10^{14}\mathrm{W/cm}^2$ and $\lambda = 800\mathrm{nm}$ ($\omega_0 = 0.057$). In abscissa: harmonic order N, with $\omega = N\omega_0$, the harmonic frequency, and ω_0 the incident electric field frequency $R_0 = 3.2\mathrm{a.u.}$

usual cases the beam is sufficiently large so that along the propagation axis z', we can again neglect the x' and y' dependencies.

The harmonic spectra of the transmitted field, denoted by E_T, possesses in theory [24], a frequency cut-off denoted by ω_c (see Fig. 4). This cut-off corresponds to the maximum return energy acquired by an electron in the field of $E(t)$, $N_m\omega = 3.17U_p + I_p$ [14]. It is then possible to filter this field around ω_c and to create a shorter and "intense" pulse denoted by E_F, thus leading to attosecond pulses through the uncertainty relation $\Delta\omega\Delta t \sim 1$ [1, 16]:

$$E_F(t) = \frac{1}{2\pi}\int_{\omega_c-\Delta\omega}^{\omega_c+\Delta\omega} \widehat{E}_T(\omega)e^{i\omega t}\,dt. \tag{2.13}$$

See for instance, [31] or [5] or [11] for the control aspects of such new pulses.

Note that, this problem constitutes typically a multiscale physical problem as the characteristic length and time of the TDSE are much smaller ($\|\mathbf{r}\| \sim 10^{-10}$m) than the Maxwell equations characteristic ones ($\lambda \sim 10^{-6}\text{m} = 1\mu\text{m}$).

2.2. Existence and regularity for the TDSE model. In this section we are interested in the existence and regularity of solutions for the TDSE (2.7). To do this, we will use the Fourier transform set of H^1:

$$H_1 = \left\{ u \in L^2(\mathbb{R}^4), \int_{\mathbb{R}^4} (1 + \|(\mathbf{r}, R)\|^2)|u(\mathbf{r}, R)|^2 d\mathbf{r}\, dR < \infty \right\} \tag{2.14}$$

From Baudouin, Kavian and Puel [9, 10], we can easily deduce that for $\mathcal{L} \in L^\infty\big(0, T; C_b^2(\mathbb{R}^4)\big)$ and if $u_0 \in H^1 \cap H_1$, then there exists a unique solution u in $C^0(0, T; H^1 \cap H_1)$ such that

$$\left(i\partial_t + \frac{\triangle_{\mathbf{r}}}{2} + \frac{\partial^2_{RR}}{m_p} + \mathcal{L}(\mathbf{r}, R, t) \right) u(\mathbf{r}, R, t) = 0, \quad u(\mathbf{r}, R, 0) = u_0(\mathbf{r}, R). \tag{2.15}$$

Furthermore, for $K > 0$ such that

$$\|V\|_{L^\infty(0,T;C_b^2(\mathbb{R}^4))} \leq K \tag{2.16}$$

then there exists $\mathrm{C}_{T,K}$ such that

$$\|u\|_{\mathcal{C}^0(0,T;H^1\cap H_1)} \leq C_{T,K}\|u_0\|_{H^1\cap H_1}. \tag{2.17}$$

Considering now (2.7), let us suppose that for all $T > 0$, $E \in L^\infty(0, T)$ and $\partial_t E \in L^1(0, T)$. The laser field interaction $yE(t)$ we consider is *a priori* non-zero in the whole space as it is defined for all $y \in \mathbb{R}$. Physically it is obviously not true, so that we will consider a function χ defined as follows: $\chi\colon (\mathbf{r}, R) \mapsto \chi(\mathbf{r}, R)$ in $C_b^2(\mathbb{R}^4)$ and $\chi(\mathbf{r}, R) = y$ on a compact set Ω_1 of $\mathbb{R}^4$ and $\chi(\mathbf{r}, R)$ is zero outside a set Ω_2 containing strictly Ω_1. Such a function can easily be constructed by convolution of y and a plateau function. Then we can prove:

Theorem 2.1. *Let us consider the following* TDSE:

$$\begin{aligned} &i\partial_t\psi(\mathbf{r}, R, t) \\ &\qquad = \left[-\frac{1}{2}\triangle_{\mathbf{r}} + V_c(\mathbf{r}, R) - \frac{1}{m_p}\partial^2_{RR} + V_i(R) - E(t)\chi(\mathbf{r}, R) \right] \psi(\mathbf{r}, R, t). \end{aligned} \tag{2.18}$$

$\forall T > 0$, suppose that $E \in L^\infty(0, T)$ and $\partial_t E \in L^1(0, T)$. Then there exists $C_T > 0$ such that, for all $\psi_0 \in H^1\cap H_1$, there exists a solution unique $\psi \in L^\infty(0, T; H^1\cap H_1)$ and

$$\|\psi(t)\|_{L^\infty(0,T;H^1\cap H_1)} \leq C_T\|\psi_0\|_{H^1\cap H_1}. \tag{2.19}$$

PROOF. The proof is based an energy estimate in $H_1 \cap H^1$ *via* a Gronwall inequality and a compactness argument to extract a convergent subsequence. As it can be derived with some elementary modifications from the proof in Ref. [10, Theorem 2.1] and is very close to existing results, for instance [19], we do not present the proof. □

The existence of solutions for the coupled Maxwell–Schrödinger system has yet to be proved; in particular the regularity of the polarization P, equation (2.9) (linking the two systems) is useful in our numerical approach. We can expect that the polarization regularity on z' comes from the incoming electric field spatial regularity. Some interesting results about this coupling can be found for instance in [18], where the existence of global smooth and weak Maxwell–Bloch solutions is presented.

3. Some Issues on the Numerical Approach

We propose in this section to give a non exhaustive description of our numerical method to approximate a 1-D version of the Maxwell–Schrödinger system presented above. In this study the electronic variable becomes y, instead of $\mathbf{r}$ in 3-D. The extension to higher dimensions can be found in [25]. We will focus here on the polarization P computation that allows the coupling between the Maxwell and TDSE and on the boundary conditions for the TDSE.

The TDSE is approximated by a finite difference Crank–Nicolson scheme in time, and the Laplace operator is approximated using a 3-point stencil. Such a scheme, allows to preserve the ℓ^2-norm and is a second order scheme and is unconditionally stable. The Yee scheme is used to solve the Maxwell equations [32] that consists in a finite difference scheme where the electric E, and magnetic B, fields are computed on two spatial and temporal staggered grids. Under a Courant–Friedrichs–Lewy (CFL) condition, this is a stable and order two scheme (see for details [25]). At this point it is important to recall that to be valid the macroscopic Maxwell equations have to be applied on a sufficiently large domain (as it is obtained by a spatial average on microscopic Maxwell equations). Typically if we denote by $\Delta z'_M$ the Maxwell space step should be such that $\Delta z'_M \times n_0^{1/3}$ is much larger than 1 but also should be smaller than $\lambda_{\min}$, with $\lambda_{\min}$ corresponding to the highest harmonics created during the HOHG process. In each Maxwell cell, a large number of molecules is included, but in practice we solve only one TDSE to determine a local polarization. The problem has then some multiple scales as $\Delta z'_M$ is much larger than Δy_S where Δy_S is the Schrödinger grid space step. Also, Δt_M is much larger than Δt_S where Δt_S, Δt_M are respectively the Schrödinger and Maxwell solver time steps. In the numerical scheme approximating the Maxwell equations, the time step is taken, for stability reasons, equal to $D\Delta z'/c$, with D a positive constant. We then set

$$\overline{N} = E\left[\frac{\Delta t_M}{\Delta t_S}\right]. \tag{3.1}$$

Now denoting by $\mathcal{S}$ the Schrödinger operator and by $\mathcal{B}$ the Maxwell operator, the global coupled numerical scheme can be written as the following splitting scheme (here written at order 1 but computed at order 2, to preserve the Maxwell and

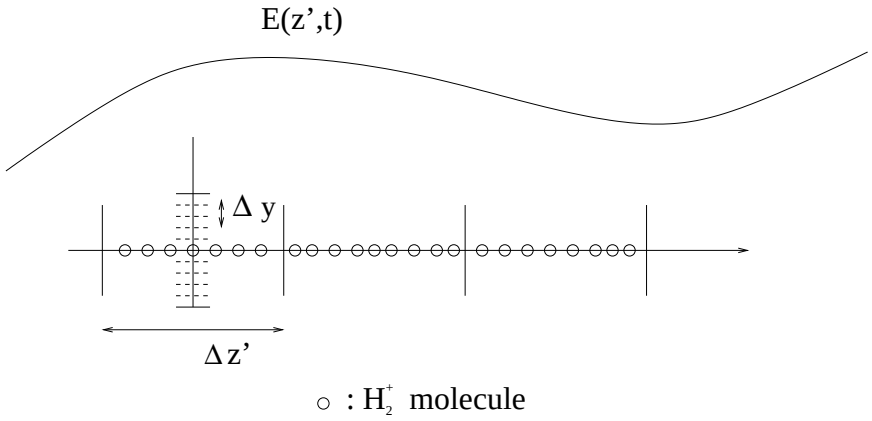

FIGURE 5. Maxwell and Schrödinger scales.

Schrödinger solvers order), from time t^n to time t^{n+1}:

$$
\left\{
\begin{array}{ll}
\mathbf{E}^{n+1} \leftarrow e^{\Delta t_M \mathcal{B}^n} \mathbf{E}^n, \ \forall z' \in [-L, L], & \\
\qquad\qquad\qquad\qquad\qquad\qquad & \text{solving the Maxwell equations,} \\
\boldsymbol{\psi}^{n+1} \leftarrow e^{[\Delta t_M - (\overline{N}-1)\Delta t_S]\mathcal{S}^n} e^{(\overline{N}-1)\Delta t_S \mathcal{S}^n} \boldsymbol{\psi}^n, & \\
\qquad\qquad\qquad\qquad\qquad\qquad & \text{solving the TDSE in each "Maxwell cell",} \\
\mathbf{P}^{n+1} \leftarrow \boldsymbol{\psi}^{n+1}, & \\
\qquad\qquad\qquad\qquad\qquad\qquad & \text{by definition of the polarization(2.9).}
\end{array}
\right. \tag{3.2}
$$

Globally, this then constitutes an order 2 scheme, stable under a CFL condition given by the Yee scheme (see [32]).

3.1. Polarization computation. The polarization computation is central in this work as it allows to couple the Maxwell equations and the TDSE. As said above the polarization is deduced from the TDSE by (2.9).

We note that for a 100 cycle laser pulse with a wavelength of 800nm interacting with molecules, we have to solve numerically at each iteration and in 1-D 8000 (80×100) TDSE's, for a Maxwell cell size equal to $10nm$ (one TDSE per Maxwell cell). As noticed above, even in 1-D, the TDSE we have to solve, because of the ion motions, are 2-D equations which is costly in CPU time. We therefore propose a technique based on a simple Taylor expansion that allows to reduce the numerical cost, assuming the polarization smooth in space. As discussed above, this assumption seems *a priori* valid when the electric field is smooth enough over dimensions (wavelength, λ) larger than molecular size (y). This satisfies also the dipole approximation, equation (2.5).

The idea is the following: we make a partition of the domain $[-\ell, \ell]$ $= \cup_{i=1,\ldots,I-1}[z_i^{'}, z_{i+1}^{'}[$ with $z_1^{'} = -l$ and $z_I^{'} = l$ and I is small integer. We suppose that each sub-domain $[z_i^{'}, z_{i+1}^{'}[$ contains a sufficiently large number of Maxwell cells. For each interval $[z_i^{'}, z_{i+1}^{'}[$, we choose a reference cell $z_{i,0}^{'}$ (located for example in the middle of the interval). For this cell we compute the corresponding TDSE which can be written in this framework:

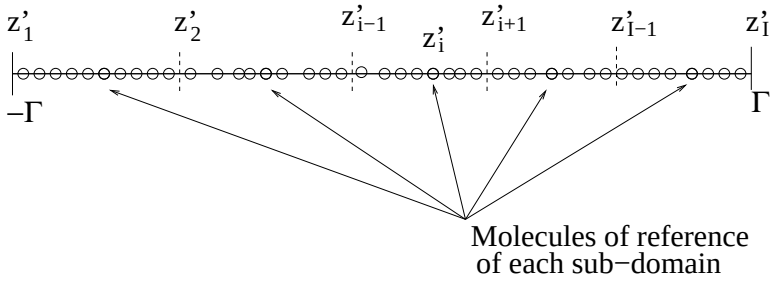

FIGURE 6. Decomposition of the domain.

$$i\partial_t \psi_{z'_{i,0}}(y,R,t) = \left(-\frac{1}{2}\partial^2_{yy} + V(y,R) - \frac{1}{m_p}\partial^2_{RR} + \frac{1}{R} + yE_{z'_{i,0}}(t)\right)\psi_{z'_{i,0}}(y,R,t). \tag{3.3}$$

and the corresponding polarization:

$$P(z'_{i,0},t) = -n(z'_{i,0})\int \psi_{z'_{i,0}}(y,R,t)\, y\, \psi^*_{z'_{i,0}}(y,R,t)\, dy\, dR. \tag{3.4}$$

An equivalent expression is obtained by using the acceleration form [14]. The present dipolar formulation is more convenient for performing a Taylor expansion as follows. Now for every other cell located in $z' \in [z'_i, z'_{i+1}[$ we have:

$$P(z',t) = P(z'_{i,0},t) + (z'-z'_{i,0})\partial_{z'}P(z'_{i,0},t) + \mathcal{O}\big((z'-z'_{i,0})^2\big). \tag{3.5}$$

Then we deduce the value of the polarization P, for every cell of the domain $[z'_i, z'_{i+1}[$. However to do this, it is necessary to compute $\partial_{z'}P(z'_{i,0},t)$. With this purpose, by differentiation in z' of (2.9), we get

$$\begin{aligned}\partial_{z'}P(z'_{i,0},t) = -n(z'_{i,0})&\int \partial_{z'}\psi_{z'_{i,0}}(y,R,t)\, y\, \psi^*_{z'_{i,0}}(y,R,t)\, dy\, dR - n(z'_{i,0})\\ &\int \psi_{z'_{i,0}}(y,R,t)\, y\, \partial_{z'}\psi^*_{z'_{i,0}}(y,R,t)\, dy\, dR - (\partial_{z'}n)(z'_{i,0})\\ &\int \psi_{z'_{i,0}}(y,R,t)\, y\, \psi^*_{z'_{i,0}}(y,R,t)\, dy\, dR.\end{aligned}$$

To compute $\partial_{z'}P(z'_{i,0},t)$ we have to compute $\partial_{z'}\psi_{z'_{i,0}}(y,R,t)$ then to solve the following equation obtained by derivation in z' of the TDSE:

$$\begin{aligned}&i\partial_t\big(\partial_{z'}\psi_{z'_{i,0}}(y,R,t)\big)\\ &\quad= \left(-\frac{1}{2}\partial^2_{yy} + V(y,R) - \frac{1}{m_p}\partial^2_{RR} + \frac{1}{R} + yE_{z'_{i,0}}(t)\right)\partial_{z'}\psi_{z'_{i,0}}(y,R,t)\\ &\qquad\qquad + iy\big(\partial_{z'}E_{z'_{i,0}}(t)\big)\psi_{z'_{i,0}}(y,R,t).\end{aligned} \tag{3.6}$$

Numerically the computation of the previous equation is very close to the computation of the TDSE.

$$\begin{aligned}\big(\partial_{z'}\psi_{z'_{i,0}}\big)^{n+1} = &\frac{(\partial_{z'}\psi_{z'_{i,0}})^{n+1}}{2} + \frac{(\partial_{z'}\psi_{z'_{i,0}})^{n}}{2}\\ &-\frac{i}{2}H^{n+1}(\partial_{z'}\psi_{z'_{i,0}})^{n+1} - \frac{i}{2}H^n\partial_{z'}\psi^n_{z'_{i,0}} + iy(\partial_{z'}E_{z'_{i,0}})^{n+1}\psi^{n+1}_{z'_{i,0}}.\end{aligned} \tag{3.7}$$

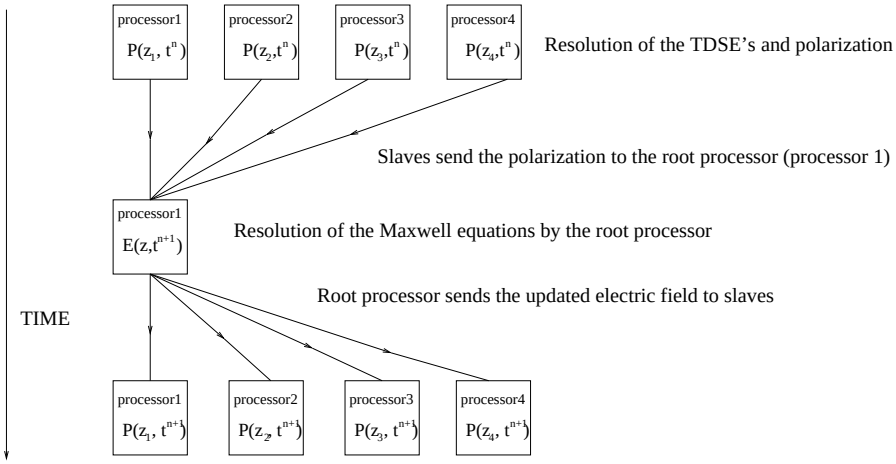

FIGURE 7. Parallelization for 4 TDSE's (molecules).

In (3.7) the quantity $\psi^{n+1}_{z'_{i,0}}$ is previously computed by the numerical scheme approximating the TDSE and with H^n naturally given by:

$$H^n = -\frac{1}{2}\partial^2_{yy} + V(y,R) - \frac{1}{m_p}\partial^2_{RR} + \frac{1}{R} + yE^n_{z'_{i,0}}, \quad n \geq 0. \tag{3.8}$$

Finally, for each sub-domain $[z_i^{'}, z_{i+1}^{'}[$ we compute $\psi_{z'_{i,0}}(y,R,t)$ and $\partial_{z'}\psi_{z'_{i,0}}(y,R,t)$ to deduce linearly from $P(z'_{i,0},t)$ the polarization for each cell located in z' of this sub-domain. The error due to this process is naturally here of order one. It is possible to increase to the second order using a higher order Taylor expansion. In this case, it would be necessary to compute $\partial^2_{z'z'}\psi_{z'_{i,0}}(y,R,t)$ obtained by double differentiation in z' of the TDSE. We can then deduce easily the following result:

Proposition 3.1. *Assuming the polarization and the molecular density smooth enough, the approximation proposed in each $z' \in [z'_i, z'_{i+1}[$, for $z' \neq z'_{i,0}$ is of order* 1 *or* 2 *depending on the Taylor expansion order.*

In practice we can expect in some cases, a strong reduction of the number of TDSE's to solve. Typically the sub-domains size will depend on the transmitted electric field E_T harmonics, then on the intensity and frequency of the incoming laser. The higher the harmonics will be, the smaller the size of the sub-domains will be chosen.

Taking into account the previous method to reduce the computational cost of the polarization, that is the number of TDSE's to solve, we have the following temporal scheme from t^n to t^{n+1}, denoting by $I-1$ the number of sub-domains, with I much smaller than the number of cells in the Maxwell grid:

$$
\left\{
\begin{array}{l}
\mathbf{E}^{n+1} \leftarrow \mathbf{E}^{n}, \quad \forall z' \in [-L, L], \\
\boldsymbol{\psi}^{n+1}_{z'_{i,0}} \leftarrow \boldsymbol{\psi}^{n}, \quad \text{for } z'_{i,0} \in [z'_i, z'_{i+1}[, \quad \forall i \in [1, I], \\
\mathbf{P}^{n+1}_{z'_{i,0}} \leftarrow \boldsymbol{\psi}^{n+1}_{z'_{i,0}} \quad \text{for } z'_{i,0} \in [z'_i, z'_{i+1}[, \quad \forall i \in [1, I], \\
\partial_{z'} \boldsymbol{\psi}^{n+1}_{z'_{i,0}} \leftarrow \boldsymbol{\psi}^{n+1}_{z'_{i,0}} \quad \text{and} \quad \text{eq. (3.6)}, \quad \text{for} \quad z'_{i,0} \in [z'_i, z'_{i+1}[, \quad \forall i \in [1, I], \\
\partial_{z'} \mathbf{P}^{n+1}_{z'_{i,0}} \leftarrow \partial_{z'} \boldsymbol{\psi}^{n+1}_{z'_{i,0}} \quad \text{for } z'_{i,0} \in [z'_i, z'_{i+1}[, \quad \forall i \in [1, I], \\
\mathbf{P}^{n+1}_{z'} \leftarrow \mathbf{P}^{n+1}_{z'_{i,0}}, \quad (\partial_{z'} n)(z'_{i,0}) \quad \text{and} \quad \partial_{z'} \boldsymbol{P}^{n+1}_{z'_{i,0}}, \quad \forall z' \in [z'_i, z'_{i+1}[, \\
\qquad\qquad\qquad\qquad\qquad\qquad\qquad\qquad \text{and} \quad \forall i \in [1, I].
\end{array}
\right. \tag{3.9}
$$

Remark on the parallelization of the polarization computation. Many approaches are possible to parallelize the Maxwell–Schrödinger equations; in particular in [25], we will present some possible issues. One of the most effective ones is as follows. To simplify the presentation let us suppose that the Maxwell-grid possesses N cells and that we solve N TDSE's (one per Maxwell-cell) with a code running on N processors. At each temporal Maxwell iteration, each processor solves one single TDSE, and computes the corresponding polarization P. Then it sends it to the root processor. The root processor "having" now the polarization in the whole physical domain, it solves the Maxwell equations (note that here our configuration the CPU cost of the Maxwell equations computation is negligible compared to the TDSE's computation cost). Then the root processor sends to the slaves the

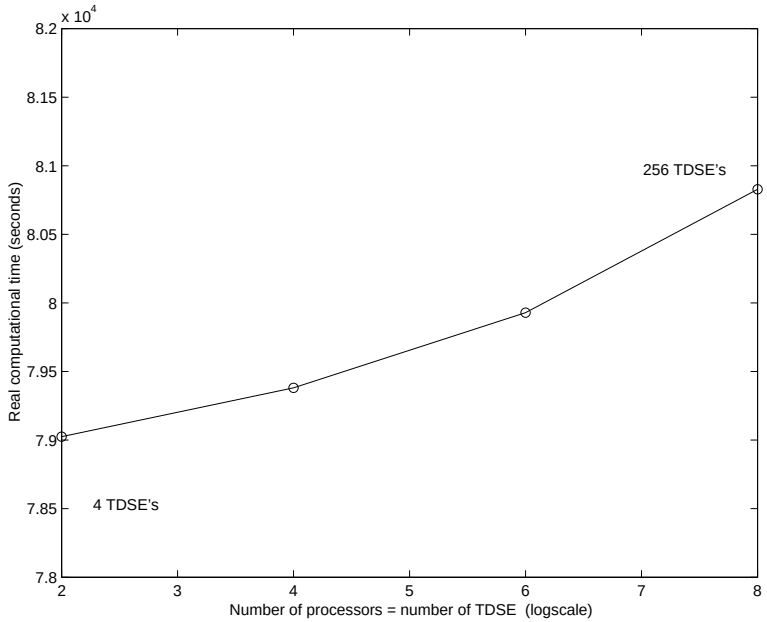

FIGURE 8. Computation of the 3-D Maxwell–Schrödinger equations with one TDSE (molecule) per processor. In ordinate the real time (in *seconds*) necessary for the numerical computation. Representation on log-scale.

updated electric field $E(t)$ (this process is summed-up in Fig. 7). Such a simple parallelization scheme allows us to obtain a very efficient speed-up. Note also that the data are distributed between the computer nodes allowing to consider a large number of molecules with sufficiently large spatial grids.

The Fig. 8 represents for a given mesh: in abscissa the number of TDSE's (4, 16, 64, 256 TDSE's) to solve also equal to the number of processors (one equation per processor) and in ordinate the real time for the 3-D code to solve the corresponding Maxwell–Schrödinger equations. The ideal configuration would be y=constant, corresponding to a speed-up equal to the number of processors. The real time of computation of our Maxwell–Schrödinger code with 256 TDSE's running on 256 processors is only 2.5% slower than the code running on 4 processors with 4 TDSE's.

The coupling of our proposed reduced computation of the polarization with this parallelization allows us to expect efficient simulations with a very large number of molecules. Note also that the parallelization is almost totally independent of the way we solve numerically the TDSE and Maxwell equations.

3.2. Boundary conditions for the TDSE. Let us now discuss the boundary conditions problem for the TDSE. The initial wavefunction (initial state) $\psi(\cdot, 0)$ support is located in the Schrödinger computational domain center. Then the laser field E interacts with the molecules and delocalizes the wavefunctions whose supports can become very large due to dissociative ionization into continuum states of both electrons and nuclei (beyond Born–Oppenheimer). Numerically it means that it is necessary to discretize the TDSE in a very large domain. To overcome this well-known problem in numerical scattering theory [6], we have to find an adapted method. The usual idea to circumvent this difficulty is to reduce the computational domain and to impose some particular numerical boundary conditions on the reduced domain. It is well-known that imposing Dirichlet or Neumann boundary conditions leads to important numerical oscillations and reflections on the boundary on the domain interacting with "physical" waves inside the domain. Absorbing boundary conditions are also used in order to absorb the numerical spurious reflections. Even if this kind of method allows effectively to reduce the spurious reflections, these are often empirical (see for instance [14] in this framework), as some "parameters" have to be adapted for each numerical situation. Moreover the spurious reflections can be made to vanish but a part of the wavefunction can also be partially or totally absorbed by the absorber. Outside the reduced domain the potential is supposed to be zero and the TDSE with laser interaction can then be solved "exactly" using for instance the Volkov state propagator [14]. As absorbing boundary conditions globally do not preserve the ℓ^2-norm of the wavefunction (as they absorb it) it can hardly be preserved. Ideally we would like to impose particular boundary conditions such that the solution of the whole space problem restricted to the compact domain (containing the solution support) is equal to the total solution on the compact domain (that is without spurious reflections). Then outside the reduced domain the wavefunction-solution is yet correct and can be updated using for instance the Volkov state propagator. To be more precise let us consider the following simplified model *without laser field*:

$$\begin{cases} (i\partial_t u + \partial_{yy}^2 u + V(y)\cdot u)(y,t) = 0, \\ u(y,0) = u_0(y), \quad u_0 \in H^1(\mathbb{R}). \end{cases} \tag{3.10}$$

We suppose that the supports of u_0 and V are strictly included in a compact set $\overline{\Omega}$. One then considers the domain $\Omega \times [0,T]$ with $\overline{\Omega} \subset \Omega$ and one denotes by Γ the boundary of Ω. One then looks for v solution of

$$\begin{cases} (i\partial_t v + \partial^2_{yy} v + V(y)\cdot v)(y,t) = 0, \quad y \in \Omega, \\ \mathcal{B}(y,\partial_y,\partial_t)v(y,t) = 0, \quad y \in \Gamma, \\ v(y,0) = u_0(y), \quad y \in \Gamma, \quad u_0 \in H^1(\mathbb{R}) \end{cases} \tag{3.11}$$

such that

$$u_{|_{\Omega\times[0,T]}} = v. \tag{3.12}$$

The main problem consists then in finding an adequate (pseudo-)differential boundary operator $\mathcal{B}$ on Γ such that (3.12) occurs. As is well-known these conditions, called Dirichlet–Neumann, are nonlocal in time (and in space in multidimension).

Denoting by $\mathbf{n}$ the outward normal of Γ and $\partial_{\mathbf{n}}$ is the trace operator on Γ we obtain:

$$\begin{cases} (i\partial_t v + \partial^2_{yy} v + V(y)\cdot v)(y,t) = 0, \quad y \in \Omega, \\ v(y,t) = -e^{i\pi/4}\displaystyle\int_0^t \frac{\partial_y v(y,\tau)}{\sqrt{\pi(t-\tau)}}\,d\tau, \quad y \in \Gamma. \end{cases} \tag{3.13}$$

This approach has been very well described in particular in [2], and some numerical issues can be found in [3,4]. We also refer to [8] for the first presented discretization of nonlocal transparent boundary conditions for the TDSE. As unfortunately these conditions are nonlocal in time, many studies have been devoted to find effective numerical approximations. At each iteration we can for instance decompose the convolution product as the sum of a local part and historical part as proposed in [21]. Thus at time t^{n+1}:

$$v(y_\Gamma, t^{n+1}) = -e^{i\pi/4}\int_0^{t^{n+1}} \frac{\partial_y v(y_\Gamma,\tau)}{\sqrt{\pi(t^{n+1}-\tau)}}\,d\tau \tag{3.14}$$

is decomposed into

$$v(y_\Gamma, t^{n+1}) = -e^{i\pi/4}\int_0^{t^n} \frac{\partial_y v(y_\Gamma,\tau)}{\sqrt{\pi(t^{n+1}-\tau)}}\,d\tau - e^{i\pi/4}\int_{t^n}^{t^{n+1}} \frac{\partial_y v(y_\Gamma,\tau)}{\sqrt{\pi(t^{n+1}-\tau)}}\,d\tau. \tag{3.15}$$

It is then possible to treat accurately each integral (see again [21]).

Coupling with the laser. Now we present some ideas related to the boundary conditions for the TDSE coupled with a laser interaction $yE(t)$. As the laser interaction does not depend on the inter-nuclear distance R, then the TDSE we consider here simply writes:

$$i\partial_t v(y,t) = \big(-\partial^2_{yy} + V(y) + yE(t)\big)v(y,t). \tag{3.16}$$

It is important to note that the term $V(y)+yE(t)$ does not have a compact support, so that it is no more possible to solve "easily" the free potential TDSE outside a bounded domain as done above. Indeed, outside a given domain containing the support of the Coulomb potential V, the potential free equation becomes:

$$i\partial_t v(y,t) = \big(-\partial^2_{yy} + yE(t)\big)v(y,t). \tag{3.17}$$

Using as above a Laplace transform in time would lead to a convolution product between the Laplace transforms of E and v. We then propose not to solve exactly this equation but to give an approximate condition based on a splitting operator. Given the solution on the boundaries at time t^n we look for it at time t^{n+1} splitting the equation (3.16):

$$\begin{cases} i\partial_t v(y,t) = yE(t)v(y,t), & y\in\Gamma,\ t\in[t^n,t^{n+1/2}[,\\ i\partial_t v(y,t) = \big(-\partial_{yy}^2 + V(y)\big)v(y,t), & y\in\Gamma,\ t\in[t^{n+1/2},t^{n+1}]. \end{cases}$$

The first equation provides the following solution:

$$v(y_\Gamma, t^{n+1/2}) = e^{-iy_\Gamma\int_{t^n}^{t^{n+1}}E(s)\,ds}v(y_\Gamma,t^n). \tag{3.18}$$

To approximate the second one we consider the solution at time t^{n+1} when the laser is *null*:

$$v(y_\Gamma,t^{n+1}) = -e^{i\pi/4}\int_0^{t^{n+1}}\frac{\partial_y v(y_\Gamma,\tau)}{\sqrt{\pi(t^{n+1}-\tau)}}\,d\tau. \tag{3.19}$$

We then decompose this integral in two parts corresponding to the local and historical parts.

$$v(y_\Gamma,t^{n+1}) = -e^{i\pi/4}\int_0^{t^n}\frac{\partial_y v(y_\Gamma,\tau)}{\sqrt{\pi(t^{n+1}-\tau)}}\,d\tau - e^{i\pi/4}\int_{t^n}^{t^{n+1}}\frac{\partial_y v(y_\Gamma,\tau)}{\sqrt{\pi(t^{n+1}-\tau)}}\,d\tau. \tag{3.20}$$

The historical part depends on v at time t^n and is then known at time t^{n+1}. For the local part we use $v(y_\Gamma,t^{n+1/2})$ in order to compute $v(y_\Gamma,t^{n+1})$. More precisely and following approximations proposed by Greengard in [21], the historical part is approximated by:

$$-e^{i\pi/4}\int_0^{t^n}\frac{\partial_y v(y_\Gamma,\tau)}{\sqrt{\pi(t^{n+1}-\tau)}} \sim -e^{i\pi/4}\sum_{j=1}^{M} w_j c_j(n), \tag{3.21}$$

where $\big(c_j(n)\big)_j$ and $(w_j)_j$ are some sequences described in [21].

The local part is then approximated by Gauss-Legendre quadrature:

$$\begin{aligned} -e^{i\pi/4}\int_{t^n}^{t^{n+1}}\frac{\partial_y v(y_\Gamma,\tau)}{\sqrt{\pi(t^{n+1}-\tau)}}\,d\tau \sim -e^{i\pi/4}\sqrt{\frac{\Delta t^{n+1}}{\pi}}(&\alpha v_{y,\Gamma}^{n+1/2}\\ &+(2-\alpha)v_{y,\Gamma}^{n}),\quad 0\le\alpha\le 2. \end{aligned} \tag{3.22}$$

With such an approach we then obtain the following boundary conditions. If J denotes the last cell index: $J\Delta y = y_\Gamma\in\Gamma$.

$$\begin{cases} v_J^{n+1} = -e^{i\pi/4}\left(\displaystyle\sum_{j=1}^{N_c} w_j c_j(n) + \sqrt{\frac{\Delta t^{n+1}}{\pi}}\left(\alpha\frac{v_J^{n+1/2}-v_{J-1}^{n+1/2}}{\Delta y}e^{-iy_\Gamma\int_{t^n}^{t^{n+1}}E(s)\,ds}\right.\right.\\ \qquad\qquad\left.\left.+(2-\alpha)\frac{v_J^n - v_{J-1}^n}{\Delta y}\right)\right),\\ c_j(n+1) = e^{s_j^2\Delta t^n}c_j(n) + \dfrac{\Delta t^n}{2}\left(e^{-s_j^2\Delta t^{n+1}}\dfrac{v_J^n - v_{J-1}^n}{\Delta y}\right.\\ \qquad\qquad\left.+e^{-s_j^2(\Delta t^n+\Delta t^{n+1})}\dfrac{v_J^{n+1}-v_{J-1}^{n+1}}{\Delta y}\right). \end{cases}$$

Where,

$$v_J^{n+1/2} = e^{-iy_\Gamma \int_{t^n}^{t^{n+1}} E(s)\,ds} v_J^n, \quad v_{J-1}^{n+1/2} = e^{-iy_\Gamma \int_{t^n}^{t^{n+1}} E(s)\,ds} v_{J-1}^n. \tag{3.23}$$

Note that by induction, the historical part depends also on the laser field E. A symmetric approach is proposed in $-y_\Gamma$. These 2 discrete equations in $-J$ and J close the Crank–Nicolson system. As a consequence the Hermitian structure of the sparse matrix is lost so that a GMRES method (see [30]) is used to solve the linear system. Our strong assumption consists then in searching for a numerical boundary condition that behaves like $\int_0^t \partial_y v(y,\tau)/\sqrt{\pi(t-\tau)}\,d\tau$. Note also that it is straightforward to apply the technique presented above in the velocity gauge.

To illustrate this technique we propose a simple benchmark on the TDSE under the Born–Oppenheimer approximation (fixed R). We assume here that the Coulomb potential is equal to zero.

$$\begin{cases} i\partial_t u(y,t) + \partial_{yy} u(y,t) + yE(t)u(y,t) = 0, \quad y \in [-10,10], \quad t \geq 0, \\ u(y,0) = u_0(y) = e^{8iy} e^{-y^2}. \end{cases} \tag{3.24}$$

The benchmark we propose is as follows. The global domain is $[-10;10]$ and the space grid τ contains 800 cells with a space step equal to 0.05. The reduced domain $\Omega = [-5,5]$ contains the initial data support. We impose the Dirichlet–Neumann boundary conditions coupled the laser as described above, at $x_{-\Gamma} = -5$ and $x_\Gamma = 5$. Outside Ω we solve the TDSE taking as boundary conditions the solution computed $x_{\mp\Gamma}$. We compare our numerical solution with the solution obtained using Dirichlet boundary conditions at $x_{-\Gamma} = -5$ and $x_\Gamma = 5$ and with a reference solution. We consider a two-cycle laser pulse, with an intensity equal to 0.05 and a duration of 0.76 (note that we use *a.u.*).

The Dirichlet–Neumann numerical (Fig. 9) solution is then far less reflected (even if a small reflection exists) than the Dirichlet solution. Here, note that the grid is coarse and small, so that the influence of spurious reflections can be obviously diminished using a larger grid and smaller space steps. Another approach to make decrease the reflections consists in making a better approximation of the historical part in the method presented above. In order to do this, it is necessary to approximate this historical integral using the solution at the boundaries at all previous times (t^n, t^{n-1}, t^{n-2}, *etc*). This then would lead to the approach of Antoine and Besse in [3] where the authors are enable to reduce drastically the spurious reflections. The price to pay is however to store the solution at the boundaries at all times, which would be problematic in higher dimensions.

We note that the benchmark we have considered above corresponds to a total ionization (the wavefunction leaves totally the reduced domain because of the wavenumber equal to 8). This is not of interest in our model at this time. Indeed we want the electrons to stay inside the domain in order to take into account the plasma effects due to free electrons.

Finally note that another approach based on the exact solution of the TDSE without Coulomb potential but with an electric field (see Volkov wavefunction) will be developed in a forthcoming paper. Typically this would involve the computation

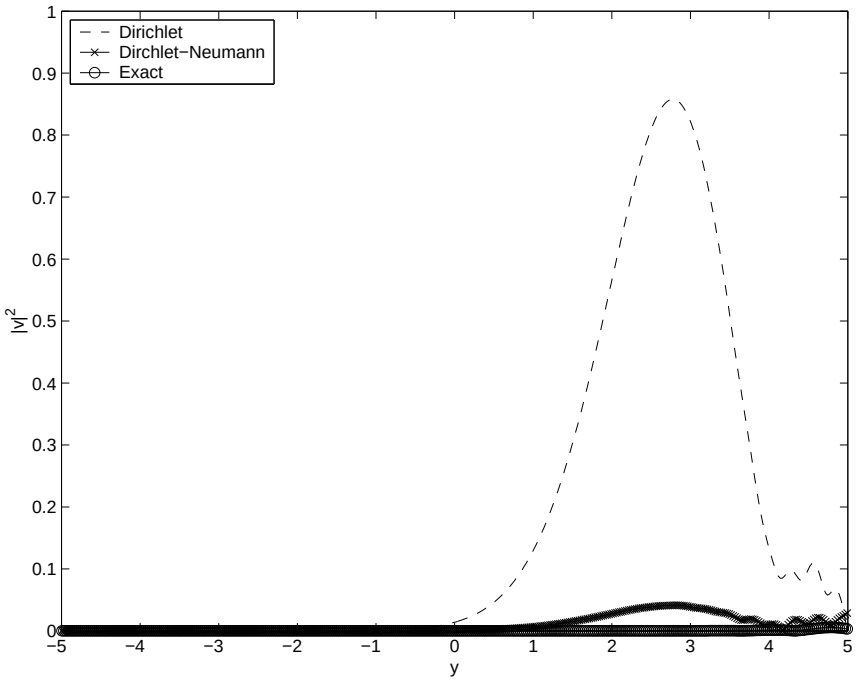

FIGURE 9. Comparison between a reference solution and the numerical solutions obtained with Dirichlet and Dirichlet–Neumann coupled with the laser.

at the boundary y_Γ of the quantity:

$$
\begin{aligned}
(3.25)\quad & v(y_\Gamma, t^{n+1}) \\
&= \frac{1-i}{2\sqrt{\pi t^{n+1}}} \exp\left(-iy_\Gamma \int_0^{t^{n+1}} E(s)\, ds - \frac{i}{2}\int_0^{t^{n+1}} \left(\int_0^s E(\tau) d\tau\right)^2 ds\right) \\
&\qquad \times \int_{\mathbb{R}} v_0(y') \exp\left(\frac{i(y_\Gamma - \int_0^{tn+1}\left(\int_0^s E(\tau)\, d\tau\right)\, ds - y')^2}{2t^{n+1}}\right) dy,
\end{aligned}
$$

corresponding to the exact solution of the TDSE without potential. Note that in the convolution product in the previous formula, we only integrate over the initial wavefunction support.

3.3. Some preliminary numerical tests. We present here two numerical results obtained when solving the Maxwell–Schrödinger equations in 1-D and 3-D. The first result Fig. 10 represents for a 1-D computation, the harmonic orders contained in the transmitted electric field $\widehat{E}(\omega)$ of intensity $|\widehat{E}(\omega)|^2$ ($\omega = N\omega_0$, with ω_0 the incident laser frequency), for a few-cycle (2–3 cycles) laser propagation in a H_2^+ medium of length equal from 14nm (corresponding to 1 TDSE), to 28.7μm (2048 TDSE's) at $R = 2$. Note that we obtain a good linear scaling of the low order harmonic intensities, when we increase the domain length, as expected for such a coherent process [15,16]. Note also that the seventh harmonics is particularly

excited as remarked in numerous computations (see [23] for instance). In this case, as the density is very small (10 Torr, that is $\sim 3.54 \times 10^{17}$mol/cm^3) the attopulse shapes are not modified (only linearly amplified) by the medium. In opposite for a much larger molecular density ($\sim 10^{20}$mol/cm^3, with the same data than above and $R = 2$) we observe a modification on Fig. 11 of the linear scaling even for low order harmonic intensities (see for instance the seventh harmonics) This phenomenon related to the fact that the wavelength of the highest harmonics approach the inter-molecule distance [25].

The second numerical result Fig. 12 is the transmitted electric field harmonics (squared) for a 3-D computation, with a 5-cycle pulse propagation in a H_2^+ media of length respectively equal to 15nm (corresponding to 4 TDSE's), 60nm (16 TDSE's), 240nm (64 TDSE's). The pressure is here equal to 640 Torr. The code was run during approximately 22 hours respectively on 4, 16 and 64 Xeon (Intel) processors (see `www.ccs.usherbrooke.ca/mammouth`). Again we remark that the computation gives us a linear scaling for the low order harmonics with respect to the propagation length. These two results show also the high order harmonic generation by the electric field acting on the H_2^+ molecules and the high intensity of some of these harmonics as a result of nonlinear non-perturbative laser-molecule interaction. This observation confirms the necessity for the use of our Maxwell–Schrödinger model instead of perturbative Maxwell–Schrödinger models to study intense ultrashort lasers behaviours in nonlinear media where ionization occurs. Indeed for these

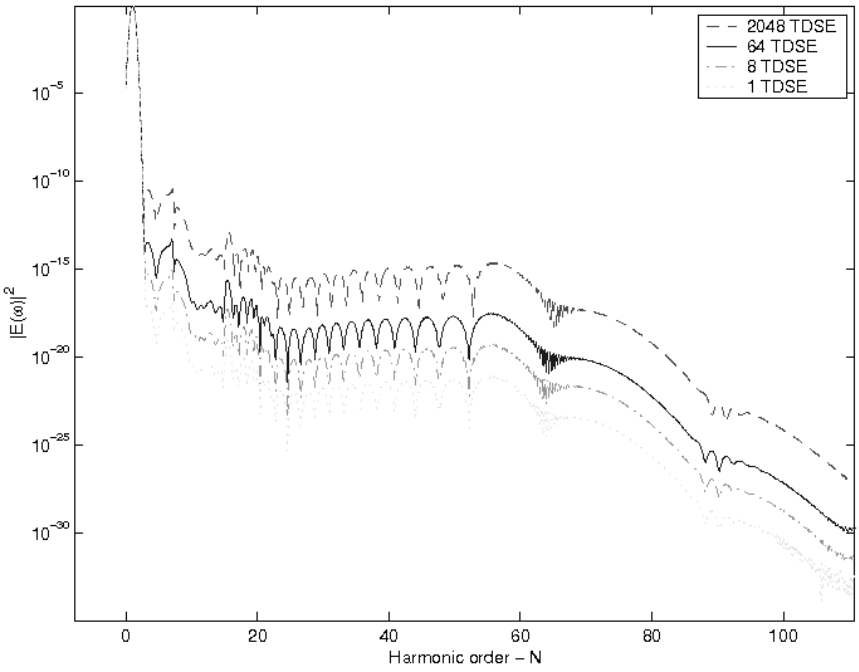

FIGURE 10. $|\widehat{E}(\omega)|^2$, for 14nm (1 molecule), 112nm (8 molecules), 896nm (64 molecules) and 28.7μm (2048 molecules) and $n_0 \sim 3.54 \times 10^{17}$mol/cm^3 in 1-D. In abscissa: harmonic order N, with $\omega = N\omega_0$ and ω_0 incident electric field frequency.

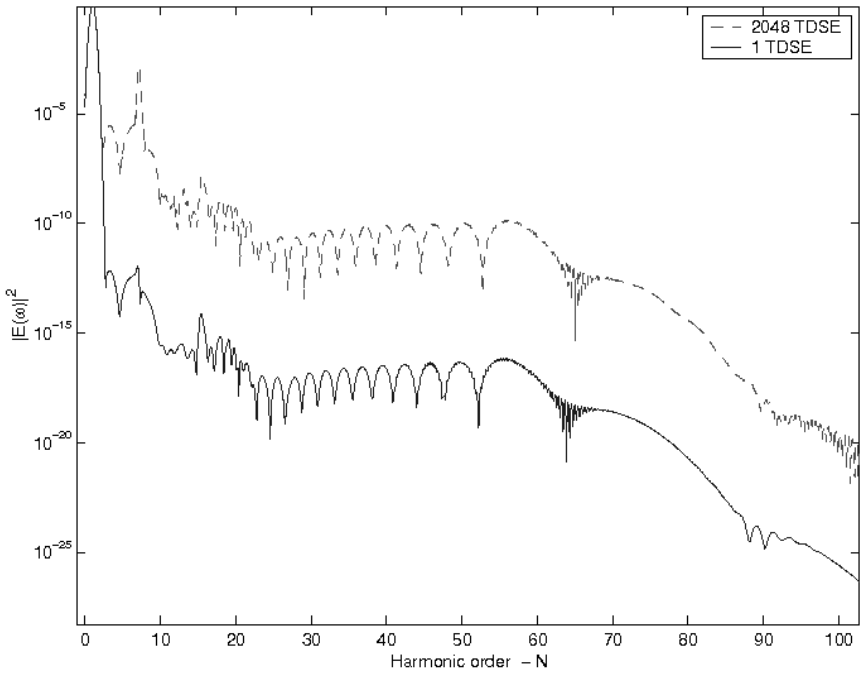

FIGURE 11. $|\widehat{E}(\omega)|^2$, for $2nm$ (1 molecule) and 4μm (2048 molecules) and $n_0 \sim 10^{20}$mol/cm^3 in 1-D. In abscissa: harmonic order N, with $\omega = N\omega_0$, harmonic frequency, and ω_0 incident electric field frequency

last models only small order harmonics are taken into account (one equation for each harmonic). Our numerical results show that higher harmonics can have an important intensity. Our model can then be for instance, an issue for filamentation [27]. Indeed, this multidimensional phenomenon is usually treated using nonlinear TDSE's (one for each harmonic) with a plasma term modeled with a nonlinear function of the electric field. However, in practice only small harmonics are taken into account and the plasma term is often poorly modeled. Finally, note that by filtering around high intense harmonics it is also possible to create shorter pulses (much higher frequency) than the incident one (2.13). See for instance that in the 3-D case, the 70th harmonics is relatively intense allowing to create by filtering an "intense" pulse of frequency 70 times larger than the incident laser one (2.13) [1]. Details of theses simulations and others will be presented in [25].

4. Conclusion

In this short paper, we have presented a Maxwell–Schrödinger model for laser-molecule interaction in the nonlinear nonperturbative regime and some aspects of its numerical computation. In particular, we have proposed some avenues to reduce the algorithmic complexity of the numerical problem due to the multiple scales (polarization computation for instance) but also due to the boundary conditions involving continuum (dissociative ionization) states both electronic and nuclear.

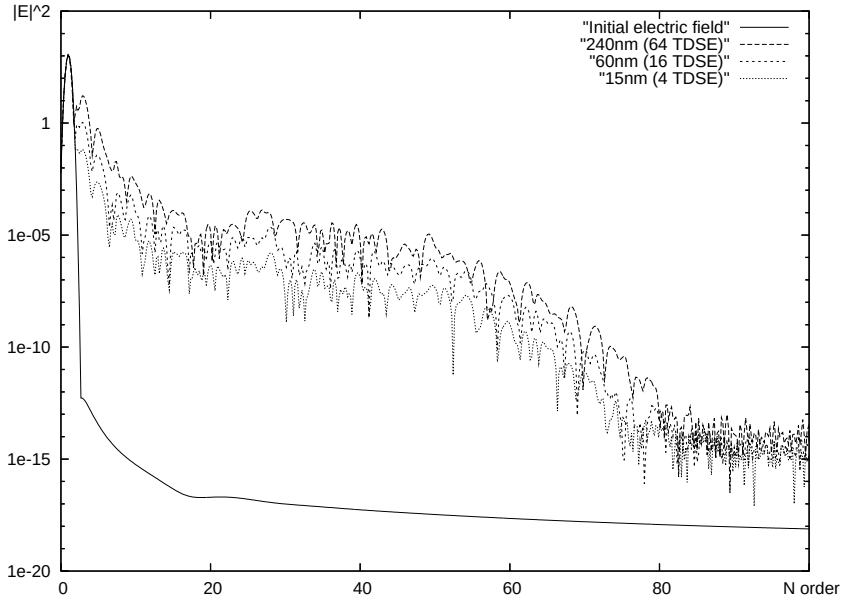

FIGURE 12. $|\widehat{E}(\omega)|^2$, for 15nm (4 molecules), 60nm (16 molecules), 240nm (64 molecules) in 3-D. In abscissa: harmonic order N, with $\omega = N\omega_0$, harmonic frequency, and ω_0 incident electric field frequency.

In this framework, we have presented a 1-D approach to manage the "dispersive" effects for the TDSE which is obviously applicable on cubic box faces in 3-D. However to overcome the difficulties due to the cubic domain singularities, a better approach consists in applying some really multi-dimensional Dirichlet–Neumann boundary conditions. Then some new numerical difficulties arise due to the fact that such conditions are non-local in space (and in time): the condition on each boundary point of the domain depends on all the points of the domain at all previous times. In [4] the authors proposed in 2-D for laser free problems to use an approximation of the Dirichlet–Neumann nonlocal pseudodifferential operator by some local differential operators (involving in particular the Beltrami operator on the boundary). They are then able to obtain order two local approximations of the "exact" nonlocal operator. In [25] we will show how we propose to apply a derivation of their technique in the framework of laser-molecule interactions. We will also focus on transversal effects, that is spatial-temporal pulse shape effects, of the laser field interacting with a gas not taken into account in this note. Another point to investigate comes from the following remark. For a 10 Torr pressure, and supposing an ideal molecular equidistribution, the space between two molecules is given by 12nm. In HOHG by a 800nm-laser, the 67th harmonic is approximately equal to $12nm$. This specific configuration, that corresponds exactly to one electric field cycle between two molecules presents challenges for the inclusion of microscopic details into Maxwell–Schrödinger equations.

References

1. P. Agostini and L.F. DiMauro, *The physics of attosecond light pulses*, Rep. Progr. Phys. **67** (2004), no. 813, 813–855.
2. X. Antoine, H. Barucq, and L. Vernhet, *High-frequency asymptotic analysis of a dissipative transmission problem resulting in generalized impedance boundary conditions*, Asymptot. Anal. **26** (2001), no. 3-4, 257–283; MR1844544 (2002e:35036)
3. X. Antoine and C. Besse, *Unconditionally stable discretization schemes of non-reflecting boundary conditions for the one-dimensional Schrödinger equation*, J. Comput. Phys. **188** (2003), no. 1, 157–175; MR1985023 (2004e:65104)
4. X. Antoine, C. Besse, and V. Mouysset, *Numerical schemes for the simulation of the two-dimensional Schrödinger equation using non-reflecting boundary conditions*, Math. Comp. **73** (2004), no. 248, 1779–1799 (electronic). MR2059736 (2005c:65067)
5. A.D. Bandrauk, S. Chelkowski, and N.H. Shon, *Nonlinear photon processes in molecules at high intensities-route to* XUV*-attosecond pulse generation*, J. Mol. Struct. **735–736** (2005), 203–209.
6. A.D. Bandrauk and S. Chelkowski, *Dynamic imaging of nuclear wavefunctions with ultrashort* UV *laser pulses*, Phys. Rev. Lett. **87** (2001), no. 27, 113–120.
7. A.D. Bandrauk and H.-Z. Lu, *Numerical methods for molecular time-dependent Schrödinger equations—bridging the perturbative to nonperturbative regime*, Handbook of Numerical Analysis, vol. X, North-Holland, Amsterdam, 2003, pp. 803–832.
8. V.A. Baskakov and A.V. Popov, *Implementation of transparent boundaries for numerical solution of the Schrödinger equation*, Wave Motion **14** (1991), no. 2, 123–128. MR1125294 (92g:78001)
9. L. Baudouin, O. Kavian, and J.-P. Puel, *Régularité dans une équation de Schrödinger avec potentiel singulier à distance finie et à l'infini*, C. R. Math. Acad. Sci. Paris **337** (2003), no. 11, 705–710. MR2030406 (2004k:35308)
10. ———, *Regularity for a Schrödinger equation with singular potentials and application to bilinear optimal control*, J. Differential Equations **216** (2005), no. 1, 188–222. MR2158922
11. A. Ben Haj-Yedder, C. Le Bris, O. Atabek, A.D. Bandrauk, and S. Chelkowski, *Optimal control of attosecond pulse synthesis from high order harmonic generation*, Phys. Rev. A **69** (2004), 041802-1–041802-4.
12. T. Brabec and F. Krausz, *Intense few-cycle laser fields*: *frontier of nonlinear optics*, Rev. Modern Phys. **72** (2000), no. 545–591.
13. S. Chelkowski, A. D. Bandrauk, and P.B. Corkum, *Muonic molecules in superintense laser fields*, Phys. Rev. Lett. **93** (2004), 083602-1–083602-4.
14. S. Chelkowski, C. Foisy, and A.D. Bandrauk, *Electron-nuclear dynamics of multiphoton* H_2^+ *dissociative ionization in intense laser fields*, Phys. Rev. A **57** (1998), no. 2, 1176–1185.
15. I. Christov, *Generation and propagation of attosecond* x*-ray pulses in gaseous media*, Phys. Rev. A **57** (1998), no. 4, 2285–2288.
16. ———, *Enhanced generation of attosecond pulses in dispersion-controlled hollow-core fiber*, Phys. Rev. A **60** (1999), no. 4, 3244–3250.
17. M. Defranceschi and C. Le Bris (eds.), *Mathematical models and methods for ab initio quantum chemistry*, Lecture Notes in Chem., vol. 74, Springer-Verlag, Berlin, 2000, pp. 95–119. MR1857459 (2003e:82002)
18. E. Dumas, *Global existence for Maxwell–Bloch systems*, J. Differential Equations **219** (2005), no. 2, 484–509. MR2183269
19. R.J. Iório, Jr. and D. Marchesin, *On the Schrödinger equation with time-dependent electric fields*, Proc. Roy. Soc. Edinburgh Sect. A **96** (1984), no. 1-2, 117–134. MR741652 (85k:35179)
20. J.D. Jackson, *Classical electrodynamics*, 2nd ed., John Wiley & Sons Inc., New York, 1975. MR0436782 (55 #9721)
21. S. Jiang and L. Greengard, *Fast evaluation of nonreflecting boundary conditions for the Schrödinger equation in one dimension*, Comput. Math. Appl. **47** (2004), no. 6-7, 955–966. MR2060329 (2004m:35217)
22. M. Jungreuthmayer, C.M. Geissler, J. Zanghelini, and T. Brabec, *Microscopic analysis of large-cluster explosion in intense laser fields*, Phys. Rev. Lett. **92** (2004), no. 13, 133401-1–133401-4.

23. G.L. Kamta and A.D. Bandrauk, *Three-dimensional time-profile analysis of high-order harmonic generation in molecules: nuclear interferences in* H_2^+, Phys. Rev. A **71** (2005), no. 5, 53407-1–19.
24. M. Lewenstein, Ph. Balcou, M. Yu, A. Huillier, and P.B. Corkum, *Theory of high-harmonic generation by low frequency laser fields*, Phys. Rev. A **49** (1994), no. 3, 2117–2132.
25. E. Lorin, S. Chelkowski, and A.D. Bandrauk, *Numerical Maxwell–Schrödinger model for intense laser-molecule interaction and propagation*, Preprint CRM (to appear).
26. A. Maimistov E. Kazantseva, and J.-G. Caputo, *Reduced Maxwell–Duffing description*, Phys. Rev. E **71** (2005), 056622-1–056622-12.
27. G. Mechain, A. Couairon, M. Franco, B. Prade, and A. Mysyrowicz, *Organizing multiple femtosecond filaments in air*, Phys. Rev. Lett. **93** (2004), no. 3, 035003.
28. S.C. Rae and K. Burnett, *Harmonic generation and phase matching in the tunnelling limit*, J. Phys. B **26** (1993), 1509–1518.
29. ———, *Generation and propagation of high-order harmonics in a rapidly ionizing medium*, Phys. Rev. A **50** (1994), 3438–3446.
30. Y. Saad and W. Schultz, GMRES: *a generalized minimal algorithm for solving nonsymmetric linear systems*, SIAM J. Sci. Static. Comput. **7** (1986), no. 3, 856–869.
31. N.H. Shon, A. Suda, and K. Midorikawa, *Generation and propagation of attosecond pulses in He gas with sub-10-fs driver pulses*, Phys. Rev. A **60** (1999), no. 3, 2587–2590.
32. K.S. Yee, *Numerical solution of initial boundary value problems involving Maxwell's equations in isotropic media*, IEEE Trans. Antennas and Propagation **AP-16** (1966), 302–307.

Centre de Recherches Mathématiques, Université de Montréal, C.P. 6128, succ. Centre-ville, Montréal, Québec, H3C 3J7, Canada.
E-mail address: lorin@CRM.UMontreal.CA

Laboratoire de Chimie Théorique, Université de Sherbrooke, Sherbrooke, Québec, J1K 2R1, Canada.
E-mail address: Szczepan.Chelkowski@USherbrooke.ca

Département de Chimie, Université de Sherbrooke, Sherbrooke, Québec, J1K 2R1, Canada.
E-mail address: Andre.Bandrauk@USherbrooke.ca